COMMUNICATION

Check for updates

Hydrophobicity and dielectric properties across an isostructural family of MOFs: a duet or a duel?†

Simona Sorbara,‡[a] Soumya Mukherjee, [iD] ‡*[b] Andreas Schneemann, [iD] [c]
Roland A. Fischer [iD] *[b] and Piero Macchi [iD] *[a]

An isoreticular family of metal–organic frameworks is post-synthetically subjected to polymer grafting. Surface hydrophobicity analysis, adsorption experiments, and impedance spectroscopy characterise the water molecules adsorbed, both on the surface and in the pores, while resolving how molecular mobility is impacted.

Metal–organic frameworks (MOFs) have emerged in the past three decades not only as new and exotic by-design structures,[1–5] but also as disruptive materials for many applications.[6,7] Their strengths stand in compositional modularity, exemplifying bottom-up design of porosity, ideal for extracting, separating, and trapping molecules.[8,9] Registering structural and mechanical functionalities akin to most commercially adopted materials, typically low MOF densities can be leveraged, making them excellent alternatives for several niche industrial sectors. If designed right, low dielectric constant (low-κ) materials can be predicated upon MOFs, fundamental for the miniaturization of integrated circuits in modern information technology.[10] MOFs can be regarded as materials that protect an empty (hence not polarizable) nanospace, through their internal surface. Coupling all these aspects with chemical, thermal, and mechanical stability,[11] makes them the perfect answers to industrial bottlenecks of the current times.[12]

However, high porosity in MOFs is often accompanied by propensity for hydrolytic dissociation, a serious pitfall coming in the way of harnessing these as low-κ materials. Only a few remediation routes exist: (a) using ligands featuring optimal

[a] *Department of Chemistry, Materials and Chemical Engineering, Polytechnics of Milan, Via Mancinelli 7, 20131 Milan, Italy. E-mail: piero.macchi@polimi.it*

[b] *Technical University of Munich (TUM), TUM School of Natural Sciences, Department of Chemistry, Chair of Inorganic and Metal–Organic Chemistry, Catalysis Research Center (CRC), Munich, Germany.*
E-mail: soumya.mukherjee@tum.de, roland.fischer@tum.de

[c] *Lehrstuhl für Anorganische Chemie I, Technische Universität Dresden, Bergstrasse 66, 01069 Dresden, Germany*

‡ S. S. and S. M. contributed equally to this work.

hydrophobicity that (often sterically) prevent water molecules from cleaving the metal–carboxylate/metal–nitrogen bonds;[13–15] (b) applying post-synthetic modifications to functionalize the MOF linkers with hydrophobic substituents;[16] (c) protect the MOF pores with other materials, often layered graphenes, producing hierarchical nano-composites.[17]

The first method is arguably most straightforward, but suffers from several drawbacks. Cost-inefficiency to prepare functionalised, exotic ligands constrains the ligand library size, narrowing down the scopes of MOF tuneability.[18] That most MOFs fail to preserve crystallinity and/or retain their structures after post-synthetic modifications imply a severe shortcoming in terms of harnessing the strategy (b). Conversely, the strategy (c), upon the right choice of building blocks and polymers, has recently demonstrated to hit the sweet spot of performance and stability.[19–22]

Albeit MOFs' early promises, their performances do not often translate into commercial adoption: the ubiquity of water and MOFs strong water affinity generally being the infamous culprits.[12] In this context, characterizing the true hydrophobicity in porous materials is imperative. In general, hydrophobicity is determined by measuring the water contact angle (WCA) on the external surface (*i.e.*, surface hydrophobicity) or by recording water sorption isotherms that bear the signature of pore hydrophobicity. Regardless of the clear need to correlate these two, surface and pore hydrophobicity remain mutually exclusive subjects, so much so that only a handful (<5) of MOFs thus far report both properties together,[14,23,24] *i.e.*, correlation remains an unmet challenge.

To address this, here we select a well-known family of four isoreticular MOFs, UiO-66[25] (defect-free, unsubstituted), $[Zr_6(\mu_3\text{-}O)_4(\mu_3\text{-}OH)_4(BDC)_6]_n$ (BDC = 1,4-benzenedicarboxylate) and its functionalised analogues UiO-66-X, with X = NH$_2$,[26] NO$_2$,[26] and (F)$_4$,[27] see Fig. 1. UiO-66-X (X = H, NH$_2$, NO$_2$) derivatives were synthesized following the defect-controlled synthesis method reported by DeStefano *et al.*,[28] while UiO-66-(F)$_4$ was prepared following the original literature from Hu *et al.*[27] Their structures belong to the *Fm*$\bar{3}$*m* space group (sodium chloride type),
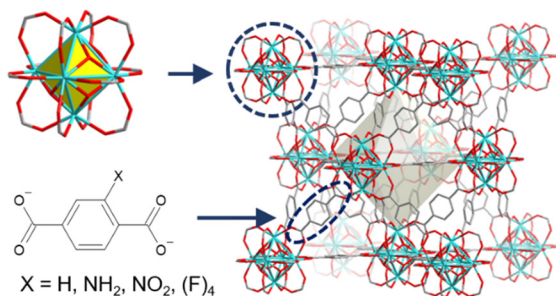
Fig. 1 The structure of UiO-66 and its isostructural derivatives, UiO-66-X (X = NH₂, NO₂, (F)₄). Top left: the secondary building unit; bottom left: formulae of the four linkers (for UiO-66-(F)₄, all four positions on the aromatic ring are fluorinated); on the right: the overall UiO-66-X architecture, including an octahedral representation of the microporous void.

see Fig. 1, where the secondary building units (SBU) occupy the unit cell vertexes and the face centres, whereas the centre of the cell (and by symmetry the midpoint of each edge) is an octahedral cavity. Hydrophilicity of these compounds are compared against the hydrophobic polymer-MOF composites (UiO-66-X-PDMS; X = H, NH_2, NO_2, $(F)_4$) we prepare, thanks to the low-cost, post-synthetic polydimethylsiloxane (PDMS) treatment (see Fig. 2; detailed characterisation: Fig. S1–S4 in the ESI†), originally reported by Zhang *et al.*[29]

To study their interactions with water molecules, two methods are the standard code of practice: water vapour adsorption isotherms (WAI), and static water contact angle (WCA) measurements. As a first foray into interlacing these two, in this work, impedance spectroscopy measurements are combined with these hydrophobicity signatures (surface: WCAs; pore: water vapour adsorption isotherms) to offer a new protocol. In essence, this three-way approach integrates all three assessments in one thread. Because of the different kinds of water sorption, the need for a multifaceted method of analysis is critical, vis-à-vis identifying physisorption (on external or internal MOF surfaces) or chemisorption (through coordination to the metal), and therefore to study their mobility and effect(s) on the materials' dielectric properties. Impedance spectroscopy, used to monitor frequency-dependent dielectric constants is not yet a standard for determining the water content adsorbed/captured in porous materials.
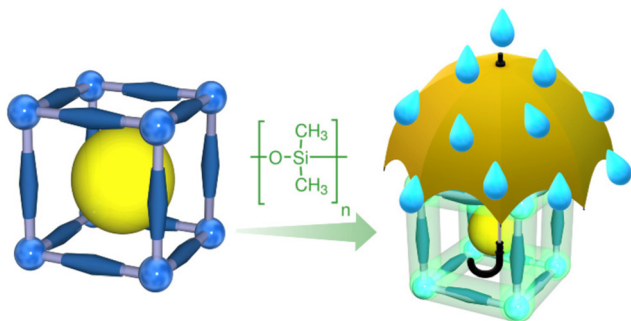
Nevertheless, reaping benefits of its high efficiency and rapidity, this tool can offer information complementary to any other acquired knowhow. In fact, thanks to frequency dependence of the applied electric field, this new approach complements the twofold insights obtained from WCA and WAI. At high frequency (in the MHz regime), the material response simply reflects the amount of polarizable electron density (MOF skeleton and pore content); at low frequency (≤ 1 Hz), the signal is sensitive to rotation and translation of the molecular dipoles free to move inside the pores and on the external surfaces. Such an arsenal of methods enables us to not only dissect the effects of hydrophobic protections in MOFs, but we also put forth a generalised hydrophobicity assessment protocol, primed to avoid fallacious conclusions in this underexplored niche.

In Fig. 3 and 4, we report the results of WAI and dielectric constant measurements on the pristine and the PDMS protected samples. PDMS treatment significantly reduces the porosity (Fig. 3 and Fig. S5, ESI†) and water vapour affinity (Fig. S6, ESI†) across this isostructural UiO-66 family. The effect is most pronounced in UiO-66-NH_2, where N_2 saturation uptake ($P/P_0 \sim 1$) is significantly (56.3%) reduced (Fig. 3d). A similar declining trend is also observed in the N_2 saturation uptakes
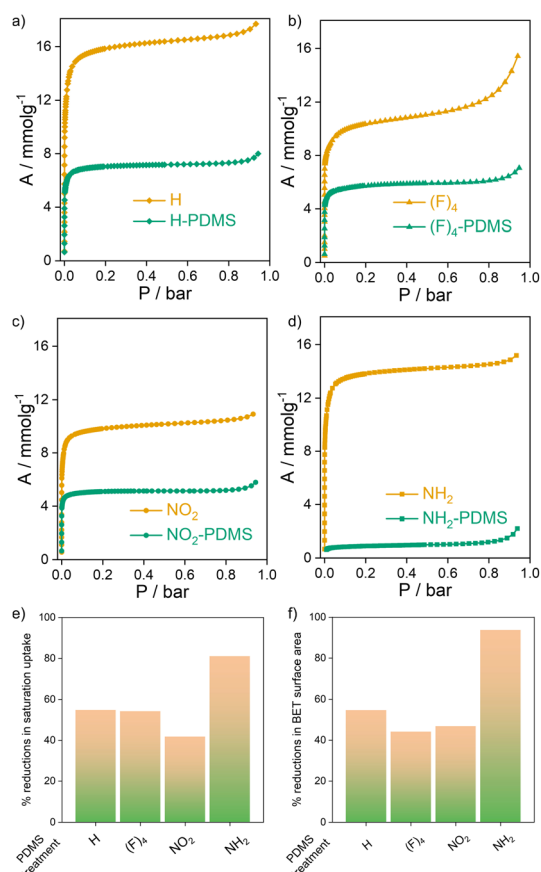

Fig. 2 General schematic illustration of the adopted PDMS protection strategy, primed to induce surface hydrophobicity in MOFs that exhibit surface hydrophilicity, pre-protection.

Fig. 3 Plots (a)–(d): comparison of N_2 adsorption isotherms for all the four UiO-66-X MOFs before and after the PDMS treatment (only the X label is shown). Plot (e): percent reduction of the nitrogen saturation uptake upon PDMS treatment. Plot (f): percent reduction of the BET surface upon PDMS treatment.
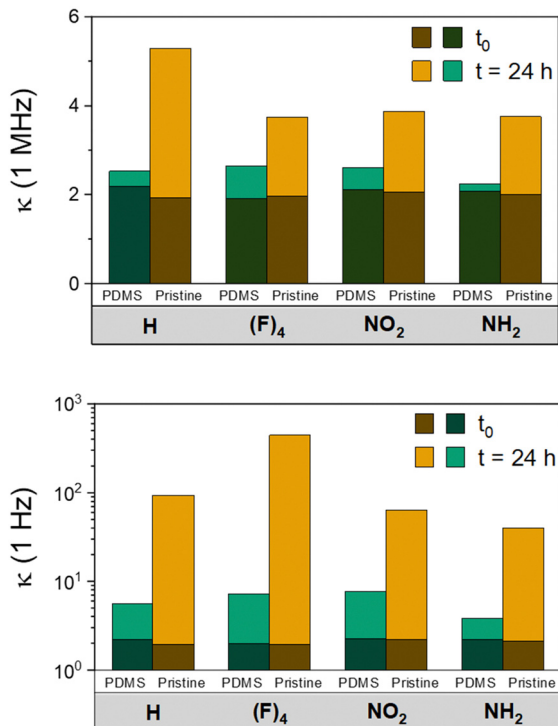
Fig. 4 Summary of the dielectric constant measurements at 1 MHz (top) and 1 Hz (bottom). For each pair, measurements were conducted on the pristine and on the PDMS protected samples, just after exposing to air (t_0) and after 24 h ($t = 24$ h). Note the small $\Delta\kappa$ observed for all the PDMS protected species (light green bars), which is especially low for X = NH2, both at 1 Hz and 1 MHz.
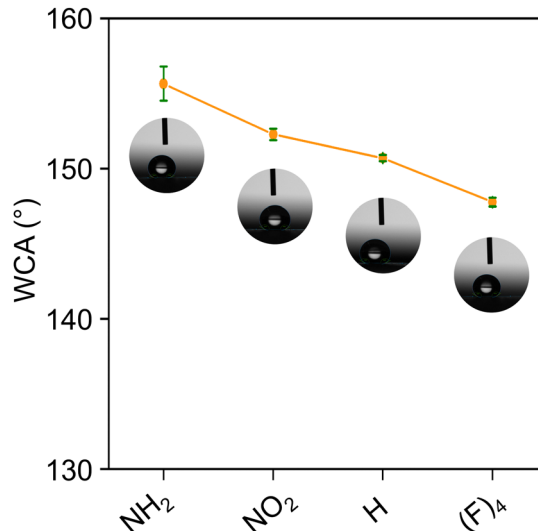

Fig. 5 Static water contact angles for the four PDMS treated UiO-66 derivatives (including the standard deviations determined from five sets of independent measurements. Insets include the water droplet pictures used for the respective measurements.

(81% for UiO-66-NH$_2$, Fig. 3f and Fig. S5 in the ESI†), and the corresponding BET surface areas (94% for UiO-66-NH$_2$, Fig. 3f).[30] Similarly, the difference between measured dielectric constant, κ, before and after 24 hours of exposure to 60% relative humidity (hereinafter, denoted as $\Delta\kappa$), is reduced by 96% at 1 Hz, and 91% at 1 MHz (Fig. 4).

The $\Delta\kappa$ trend along the PDMS treated UiO-66-X family is full of information: at 1 Hz, $\Delta\kappa$ = 1.6, 3.4, 5.2, and 5.4 for X = NH$_2$, H, (F)$_4$ and NO$_2$, respectively, whereas the analogous values at 1 MHz are, $\Delta\kappa$ = 0.2, 0.3, 0.7, and 0.5, respectively. The high frequency measurements compare well with the WAI results, projecting UiO-66-NH$_2$-PDMS as the most hydrophobic material and the one where PDMS treatment succeeded the most. At low frequency, κ reveals degree of mobility of the (undesired) guest molecules, rather than their amount. Here, the $\Delta\kappa$ reduction percentage is very similar for all the species (>90%), mostly due to the fact that for the pristine MOFs, κ increases sharply at low frequency, with no reliance upon the amount of adsorbed water (see Fig. S7 of the ESI†).

The last analysis concerns evaluation of WCAs, reported in Fig. 5. For all the unprotected UiO-66-X samples, the contact angle is not measurable because of immediate and complete adsorption of the water drop. In all the pristine phases, WCA is virtually null, which makes it impossible to rank the MOFs skeleton. After PDMS treatment, hydrophobic WCAs are registered across all UiO-66-X-PDMS variants with the decreasing

trend: UiO-66-NH$_2$-PDMS (155.7) > UiO-66-NO$_2$ (152.3) > UiO-66 (150.7) > UiO-66-(F)$_4$ (147.8) (parentheses include the static WCAs in degrees, whereas Fig. 5 includes the respective standard deviations from five sets of independent measurements). Over and above determining the highest hydrophobicity in UiO-66-NH$_2$-PDMS, rather counterintuitively, this trend is not found in perfect agreement with the dielectric constant measurements. Qualitative agreement is found with the WAI results, nonetheless. WAI is found to rely only marginally on the surface (external) hydrophobicity, whereas κ at 1 MHz evidently reflects water increase within the pores (internal). Conversely, κ at 1Hz is affected by water mobility on external surfaces and the internal channels, likely reflecting the surface phenomena only in part. These discrepancies highlight the need of combining measurements to fully characterise hydrophobicity in porous materials, with far-reaching implications beyond MOFs. In Fig. 6, we schematically compare the three techniques in terms of their ability to capture the interactions between water molecules and the porous materials. Little knowledge and statistics available on dielectric constants of MOFs preclude us to deliver a strict correlation with the amount of water molecules adsorbed. In hindsight, relying upon differences among the polarizable MOF-guest molecule interactions, increase of κ may follow a distinct trend in two different MOFs.

Herein, we inaugurate the combination of three types of measurements (water contact angle, dielectric constant, and water vapour adsorption) as an efficient approach to navigate hydrophobicity in MOFs. That each technique has its own range of sensitivity to water molecules (relying upon the surface and/or pore behaviour) imply the likelihood of translating this approach to any hydrophobic porous solids, indeed beyond MOFs.[22,31–34] Harnessing the frequency dependence of material response, recorded dielectric constant profile augments high sensitivity to both external and internal surfaces. At high

Fig. 6 Chart summarising the responses obtained from the adopted techniques, in a bid to correlate several features with pore and/or surface hydrophobicity in MOFs.

frequency, the dielectric constant reflects the water molecules residing in the solid, primarily driven by adsorption (at pores and/or surfaces). Conversely, low frequency may better reveal the presence of surface-adsorbed molecules (more mobile) from those absorbed (less mobile). To be superhydrophobic, a solid should assume the tripartite combination of (1) low water penetration on the surface (hence, very high WCA); (2) low uptake (hence, negligible water vapour uptake, and small κ at high frequency); (3) very low mobility (small κ at low frequency). Also, exemplified by the UiO-66 family of MOFs we examine herein, we demonstrate success in achieving super-hydrophobicity and high water tolerance by post-synthetic treatment with the low-cost polymer, PDMS. While analysing the determinant variables in the reduced sorption capacity, admittedly, one cannot rule out pore blocking caused by PDMS treatment, but only future studies can underpin the distinct contributions from a wider spectrum of surface and/or pore influences.

Conflicts of interest

The authors have no conflicts of interest to declare.

Notes and references

1 B. F. Hoskins and R. Robson, *J. Am. Chem. Soc.*, 2002, **112**, 1546–1554.
2 H. Li, M. Eddaoudi, T. L. Groy and O. M. Yaghi, *J. Am. Chem. Soc.*, 1998, **120**, 8571–8572.
3 S. Kitagawa, R. Kitaura and S. Noro, *Angew. Chem., Int. Ed.*, 2004, **43**, 2334–2375.
4 C. Serre, F. Millange, C. Thouvenot, M. Nogues, G. Marsolier, D. Louer and G. Ferey, *J. Am. Chem. Soc.*, 2002, **124**, 13519–13526.
5 S. L. Griffin and N. R. Champness, *Coord. Chem. Rev.*, 2020, **414**, 213295.
6 B. Hosseini Monjezi, K. Kutonova, M. Tsotsalas, S. Henke and A. Knebel, *Angew. Chem., Int. Ed.*, 2021, **60**, 15153–15164.
7 S. Mukherjee, A. V. Desai and S. K. Ghosh, *Coord. Chem. Rev.*, 2018, **367**, 82–126.
8 S. Rojas and P. Horcajada, *Chem. Rev.*, 2020, **120**, 8378–8415.
9 S. Mukherjee, D. Sensharma, O. T. Qazvini, S. Dutta, L. K. Macreadie, S. K. Ghosh and R. Babarao, *Coord. Chem. Rev.*, 2021, **437**, 213852.
10 M. Usman and K.-L. Lu, *NPG Asia Mater.*, 2016, **8**, e333–e333.
11 A. J. Howarth, Y. Liu, P. Li, Z. Li, T. C. Wang, J. T. Hupp and O. K. Farha, *Nat. Rev. Mater.*, 2016, **1**, 15018.
12 Z. Chen, M. C. Wasson, R. J. Drout, L. Robison, K. B. Idrees, J. G. Knapp, F. A. Son, X. Zhang, W. Hierse, C. Kuhn, S. Marx, B. Hernandez and O. K. Farha, *Faraday Discuss.*, 2021, **225**, 9–69.
13 T. H. Chen, I. Popov, O. Zenasni, O. Daugulis and O. S. Miljanic, *Chem. Commun.*, 2013, **49**, 6846–6848.
14 S. Mukherjee, A. M. Kansara, D. Saha, R. Gonnade, D. Mullangi, B. Manna, A. V. Desai, S. H. Thorat, P. S. Singh, A. Mukherjee and S. K. Ghosh, *Chem. – Eur. J.*, 2016, **22**, 10937–10943.
15 C. Yang, U. Kaipa, Q. Z. Mather, X. Wang, V. Nesterov, A. F. Venero and M. A. Omary, *J. Am. Chem. Soc.*, 2011, **133**, 18094–18097.
16 J. G. Nguyen and S. M. Cohen, *J. Am. Chem. Soc.*, 2010, **132**, 4560–4561.
17 K. Jayaramulu, F. Geyer, M. Petr, R. Zboril, D. Vollmer and R. A. Fischer, *Adv. Mater.*, 2017, **29**, 1605307.
18 T.-H. Chen, I. Popov, W. Kaveevivitchai and O. Š. Miljanić, *Chem. Mater.*, 2014, **26**, 4322–4325.
19 C. Petit, B. Mendoza and T. J. Bandosz, *Langmuir*, 2010, **26**, 15302–15309.
20 K. Jayaramulu, K. K. Datta, C. Rosler, M. Petr, M. Otyepka, R. Zboril and R. A. Fischer, *Angew. Chem., Int. Ed.*, 2016, **55**, 1178–1182.
21 D. D. Chronopoulos, H. Saini, I. Tantis, R. Zboril, K. Jayaramulu and M. Otyepka, *Small*, 2022, **18**, e2104628.
22 S. Mukherjee, K. K. R. Datta and R. A. Fischer, *Trends Chem.*, 2021, **3**, 911–925.
23 A. Hazra, S. Bonakala, S. A. Adalikwu, S. Balasubramanian and T. K. Maji, *Inorg. Chem.*, 2021, **60**, 3823–3833.
24 S. Roy, V. M. Suresh and T. K. Maji, *Chem. Sci.*, 2016, **7**, 2251–2256.
25 J. H. Cavka, S. Jakobsen, U. Olsbye, N. Guillou, C. Lamberti, S. Bordiga and K. P. Lillerud, *J. Am. Chem. Soc.*, 2008, **130**, 13850–13851.
26 M. Kandiah, M. H. Nilsen, S. Usseglio, S. Jakobsen, U. Olsbye, M. Tilset, C. Larabi, E. A. Quadrelli, F. Bonino and K. P. Lillerud, *Chem. Mater.*, 2010, **22**, 6632–6640.
27 Z. Hu, Y. Peng, Z. Kang, Y. Qian and D. Zhao, *Inorg. Chem.*, 2015, **54**, 4862–4868.
28 M. R. DeStefano, T. Islamoglu, S. J. Garibay, J. T. Hupp and O. K. Farha, *Chem. Mater.*, 2017, **29**, 1357–1361.
29 W. Zhang, Y. Hu, J. Ge, H.-L. Jiang and S.-H. Yu, *J. Am. Chem. Soc.*, 2014, **136**, 16978–16981.
30 S. Brunauer, P. H. Emmett and E. Teller, *J. Am. Chem. Soc.*, 1938, **60**, 309–319.
31 K. Jayaramulu, F. Geyer, A. Schneemann, S. Kment, M. Otyepka, R. Zboril, D. Vollmer and R. A. Fischer, *Adv. Mater.*, 2019, **31**, e1900820.
32 L. H. Xie, M. M. Xu, X. M. Liu, M. J. Zhao and J. R. Li, *Adv. Sci.*, 2020, **7**, 1901758.
33 Q. Zeng, H. Zhou, J. Huang and Z. Guo, *Nanoscale*, 2021, **13**, 11734–11764.
34 Y. Liu, W. Li, C. Yuan, L. Jia, Y. Liu, A. Huang and Y. Cui, *Angew. Chem., Int. Ed.*, 2022, **61**, e202113348.